

Fragment Deconstruction of Small, Potent Factor Xa Inhibitors: Exploring the Superadditivity Energetics of Fragment Linking in Protein–Ligand Complexes**

Marc Nazaré,* Hans Matter,* David W. Will, Michael Wagner, Matthias Urmann, Jörg Czech, Herman Schreuder, Armin Bauer, Kurt Ritter, and Volkmar Wehner

Predictable thermodynamic additivity is one of the cornerstones of classical covalent chemistry, allowing accurate calculation of energy terms for complete processes by addition of terms for individual components. However this principle breaks down in complex noncovalent systems, such as biological systems, in which the energetics of individual components are not truly independent of each other. This complicates predicting protein structure and folding and, the focus of this work, the prediction of ligand binding to proteins. Molecular recognition in protein–ligand complexes predominantly occurs through multiple noncovalent interactions, whereas their contribution to the total free-energy of binding (ΔG) is often unevenly distributed over the contact interface.^[1] The identification of ligands as “molecular anchors” for high affinity regions in proteins (“hot spots”) is fundamental for fragment-based drug discovery,^[2,3] indicating the similarity of ligand- and protein-centric concepts. Often high-affinity ligands encompass more than one fragment in proximal protein sites; in a few cases, individual fragments in two neighboring sites could be linked to result in high binding affinity.^[4] Ideally, the ΔG of linked fragments should be significantly greater than the sum of ΔG increments from each fragment. This overproportional increase (“superadditivity”) is attributed to the fact that each fragment loses a significant part of its rigid body rotational and translational entropy upon complex formation.^[5] Thus, the sum of ΔG for two fragments includes two unfavorable rigid body entropy barrier terms, whereas the joined molecule is only affected by one of these terms. Any ligand has to overcome this barrier because of entropy loss upon association to its site. The non-additivity for ΔG contributions is defined as linker coefficient E corresponding to the difference between the sums of fragment affinity and the final ligand [Eq. (1)].^[6]

$$\Delta G_{\text{final}} = \Delta G_{\text{frag1}} + \Delta G_{\text{frag2}} + \Delta G_{\text{link}} \quad \text{with } \Delta G_{\text{link}} = RT \ln E \quad (1)$$

Quantitative estimations for the rigid body entropy barrier were derived earlier; it was estimated as 15–20 kJ mol^{−1} at 298 K, which corresponds to three orders of magnitude in affinity.^[7] Although much has been discussed about contributions of fragment linkage to affinity, only a few examples with quantitative data have been reported so far.^[7–11] For example, nonadditive effects between hydrophobic contacts and hydrogen bonds in thrombin inhibitors were shown to depend on dynamic properties of protein–ligand complexes.^[8c]

Here we explore ΔG additivity using two series of small, but very potent inhibitors of a well-characterized and rigid protease as model system. This system allowed us to systematically investigate the energetic impact of the linker by a deconstruction analysis into fragments addressing proximal binding sites.^[12]

We recently reported indole-2-carboxamide inhibitors of the serine protease factor Xa (fXa) as central enzyme in the blood coagulation cascade.^[13] Further investigation then led to a new series of high-affinity inhibitors on a simple 2-amino-ethanesulfonamide scaffold.^[14] Potent fXa inhibitors usually contain a preorganized scaffold, which directs two vectors towards the proximal subpockets S1 and S4 as recognition “hot spots”.^[13,15] Both series share similar fragments and binding modes addressing S1 and S4 pockets. In contrast, different linkers were employed with the rigid indole-2-carboxamide and flexible 2-amino-ethanesulfonamide, which allows investigating key determinants of non-additivity because of linkers and the critical number of cooperative interactions and functional groups for binding.

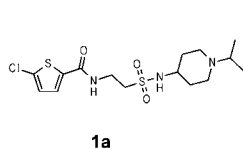
As fXa ligands with an aryl chlorine atom often favorably interact with Tyr228,^[13,16–18] we employed this S1 fragment in our deconstruction analysis. Furthermore isopropyl-4-amino-piperidine interacts through cation π interactions^[19,20] and was thus selected as minimal S4 fragment, where energetic contributions were quantified by stepwise N-alkylation.^[21,22]

Connecting attachment vectors for these motifs in S1 and S4 with a flexible 2-amino-ethanesulfonamide linker resulted in **1a** with a K_i of 2 nM (Scheme 1 and Table 1). The remarkable affinity ($\Delta G = -49.6$ kJ mol^{−1}) for one of the smallest fXa inhibitors known today^[23] with only 24 heavy atoms corresponds to a ligand efficiency of 0.49 (LE; calculated by dividing ΔG by the number of heavy atoms), suggesting that it binds with nearly optimal fit. The second arrangement of S1 and S4 motifs is represented by the indole-

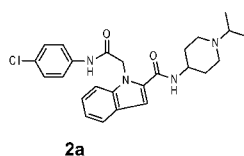
[*] Dr. M. Nazaré, Dr. H. Matter, Dr. D. W. Will, Dr. M. Wagner, Dr. M. Urmann, Dr. J. Czech, Dr. H. Schreuder, Dr. A. Bauer, Dr. K. Ritter, Dr. V. Wehner
Sanofi-Aventis Deutschland GmbH, R&D
Industriepark Höchst, Building G878
65926 Frankfurt am Main (Germany)
E-mail: marc.nazare@sanofi-aventis.com
hans.matter@sanofi-aventis.com

[**] We thank L. Bayer, S. Granata, A. Sihorsch, and S. Herok-Schöpper for synthetic assistance, V. Brachvogel, A. Liesum, and P. Lönze for support with X-ray structure determination, and Dr. M. Lorenz for discussions.

Supporting information for this article is available on the WWW under <http://dx.doi.org/10.1002/anie.201107091>.



2-Amino-ethanesulfonamide



Indole-2-carboxamide

Scheme 1. FXa inhibitors used in the deconstruction analysis.

2-carboxamide **2a**.^[13] This more rigid structure displays a ΔG value of $-48.6 \text{ kJ mol}^{-1}$ ($K_i = 3 \text{ nM}$); its LE is significantly lower (0.36).

The X-ray structure of **1a** with human fXa at a resolution of 2.40 \AA (PDB 4A7I, see the Supporting Information) confirmed our hypothesis with chlorothiophene in S1 and isopropyl piperidine in S4 (Figure 1 A) similar to indole-2-carboxamides (e.g. 2BOH^[13]). The chlorine atom is involved in nonbonded interactions with Tyr228. The ligand C=O is H-bonded to Gln192-Ne (3.06 \AA) and two water molecules

Table 1: Structures, factor Xa inhibition constants (K_i), and free-energies of binding (ΔG) for fXa inhibitors from two series in comparison to reference molecules **1a** and **2a**.^[a]

Entry	2-Amino-ethanesulfonamide series		K_i	ΔG	LE	Indole-2-carboxamide series		K_i	ΔG	LE
a		1a	0.002	−49.6	0.49		2a	0.003	−48.6	0.36
b		1b	2993	−14.4	0.18		2b	0.78	−34.9	0.32
c		1c	8% ^[b]	−11.4 ^[c]	0.18		2c	13% ^[b]	−11.4 ^[c]	0.19
d		1d	21% ^[b]	−11.4 ^[c]	0.19		2d	16% ^[b]	−11.4 ^[c]	0.21
e		1e	18% ^[b]	−11.4 ^[c]	0.27		2e (= 1e)	18% ^[b]	−11.4 ^[c]	0.27
f		1f	62.28	−24.0	0.36		2f	29.63	−25.8	0.25
g		1g	57.68	−24.2	0.58		2g	325.76	−20.0	0.43
h	n.d. ^[d]	n.d. ^[d]	n.d.	n.d.	n.d.		2h	281.22	−20.3	0.22
i	n.d. ^[d]	n.d. ^[d]	n.d.	n.d.	n.d.		2i	34% ^[e]	−15.4 ^[f]	0.18

[a] K_i values are given in μM . ΔG values are given in kJ mol^{-1} , they are calculated at 298 K. Ligand efficiencies (LE) are given in $\text{kJ}/(\text{mol} \times \text{number of non-H atoms})$; LE is calculated by dividing the free energy of binding by the number of heavy atoms in a molecule. [b] Percent inhibition observed for the corresponding fragment at a 10 mM concentration. [c] Estimated ΔG at 298 K for very weak binders from assuming a K_i value $> 10 \text{ mM}$. [d] n.d. = Not determined. [e] Percent inhibition observed for the corresponding fragment at 1 mM concentration. [f] Estimated ΔG at 298 K for very weak binders from assuming a K_i value $> 2 \text{ mM}$.

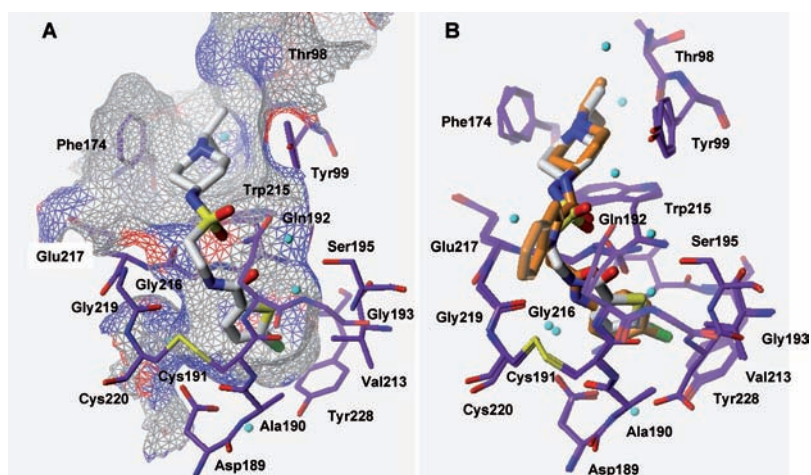


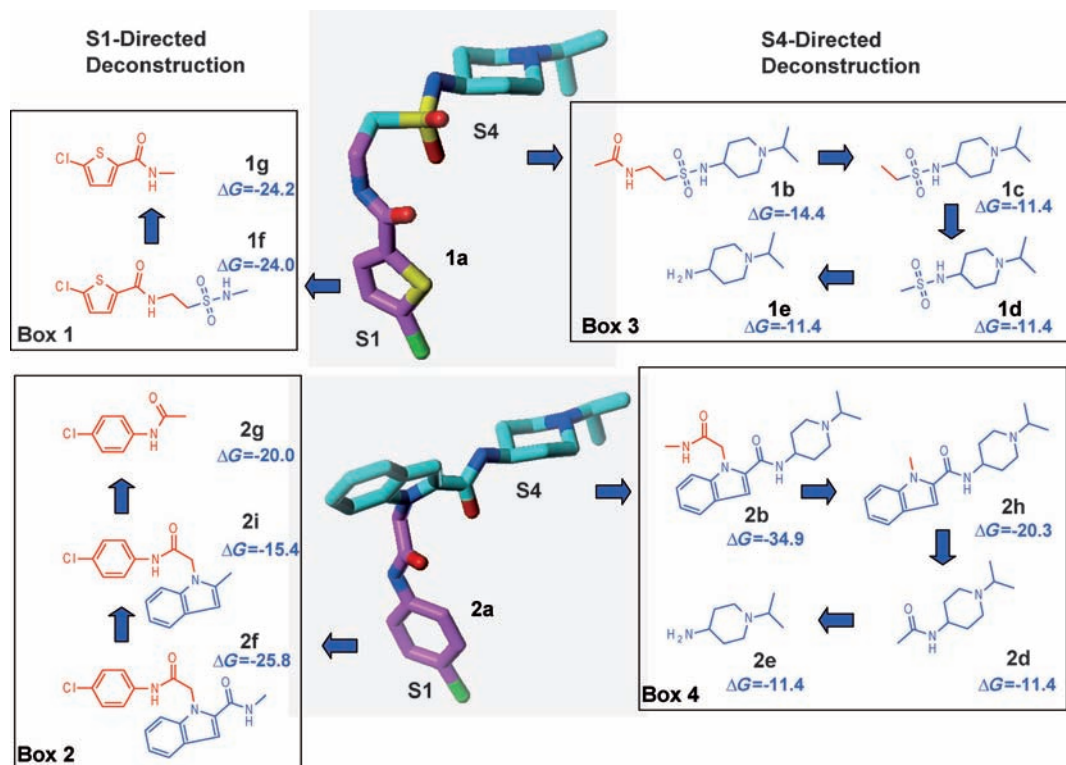
Figure 1. A) X-ray structure of 2-amino-ethanesulfonamide **1a** (K_i : 2 nM, resolution 2.40 Å, PDB 4A7I) in complex with human factor Xa. Only selected residues from fXa are shown. The binding site is indicated using a MOLCAD^[28] H-bonding surface. Crystallographic water is indicated by cyan spheres. B) Comparison of X-ray structures of **1a** (gray carbon atoms, K_i : 2 nM, 2.40 Å) and indole-2-carboxamide **2a** (orange carbon atoms, K_i : 3 nM, 2.95 Å, PDB 2BQW^[13]) with human factor Xa.

(2.75 Å each), which also interact with the catalytic Ser195-O γ plus Ser214-C=O or Gly193-NH/Ser195-NH from the oxy anion hole. The ligand amide nitrogen interacts with Gly219-C=O (3.08 Å). Both ligand sulfonamide oxygen atoms are involved in H bonds to either the Gly216-NH (2.86 Å) or the Gln192 side chain nitrogen (2.94 Å). The potential destabilizing effect of aligned dipoles of the C=O and one S=O vector is compensated by the bifurcated hydrogen bond to

Gln192-N ϵ . The isopropyl piperidine fills the S4 pocket with its protonated amine^[24] in a cation π interaction with the S4 box with distances of 4.6, 4.9, and 4.7 Å to the centroids of Phe174, Trp215, and Tyr99. The X-ray structure of fXa with the indole-2-carboxamide **2a** (PDB 2BQW, 2.95 Å)^[13] reveals a related binding mode with the acetamide NH bonded to Gly219-C=O (Figure 1B). The indole ring is packed against the Gln192 side chain, which allows a H bond between the indole-2-carboxamide oxygen and Gln216-NH.

Experimental deconstruction^[12,25,26] of both inhibitors provided insights into affinity contributions and linker influences on ΔG and LE. Scheme 2 summarizes our strategy for **1a** and **2a** to arrive at successively smaller fragments, which were synthesized and tested for fXa inhibition in a biochemical assay (Table 1).^[13,16]

The first interesting result from S4-directed deconstruction (Table 1, Scheme 2: boxes 3 and 4) is that all shorter isopropyl piperidine fragments (**1c–e** and **2c–e**) display no significant affinity at a concentration of 10 mM, regardless of whether they contain an amide or sulfonamide linkage; their inhibition is between 8–21 % ($\Delta G \gg -11$ kJ mol⁻¹, LE < 0.18 up to < 0.27), whereas the determination of K_i values was prevented at very high concentrations because of solubility limits.



Scheme 2. Fragment deconstruction process (ΔG values are given in kJ mol⁻¹).

Although the chloro thiophene **1g** displays a ΔG value of $-24.2 \text{ kJ mol}^{-1}$, this small S1 fragment with 10 heavy atoms shows a LE of 0.58, which qualifies it for fragment growth. (Scheme 2, box 1). Adding the ethanesulfonamide results in **1f** with a comparable ΔG of $-24.0 \text{ kJ mol}^{-1}$ to **1g**, whereas the LE decreased to 0.36. No favorable effect of this larger fragment is observed despite the presence of both H bond acceptors in the sulfonamide.

Deconstructing the reference inhibitor **2a** (Scheme 2, box 2) results in the S1 *para*-chloroaniline amide **2g** with a ΔG value of $-20.0 \text{ kJ mol}^{-1}$ and a LE of 0.43. Interestingly, this small fragment is less active and has a lower LE than **1g** from the 2-amino-ethanesulfonamide series with a reversed amide bond orientation. Addition of the indole to **2g** results in **2i** with lower affinity ($\Delta G \gg -15.4 \text{ kJ mol}^{-1}$) and decreased LE (< 0.18). Replacing the 2-methyl substituent in **2i** by a *N*-methyl-carboxamide results in **2f** with improved ΔG of $-25.8 \text{ kJ mol}^{-1}$, but still lower LE (0.25) compared to **2g** (0.43). This improvement in affinity could partially be attributed to favorable hydrophobic interactions of the indole to the Gln192 side chain, whereas the positive effect of the carboxamide is obvious by comparing **2f** and **2i**. These favorable interactions to the lipophilic portion of the flexible Gln192 side chain are not present in the amino-ethanesulfonamide **1f**. Shorter fragments with motifs from S4 (**2c–e**) are not active at a concentration of 10 mM. The inhibition is between 13–18%, ($\Delta G \gg -11 \text{ kJ mol}^{-1}$, LE < 0.19 up to < 0.27).

Adding the indole to the inactive S4 fragment **2d** (Scheme 2, box 4) improves ΔG in **2h** ($-20.3 \text{ kJ mol}^{-1}$, LE 0.22). The addition of a carboxamide to the indole-*N*¹-methyl leads to a significant improvement in **2b** ($\Delta G = -34.9 \text{ kJ mol}^{-1}$, LE 0.32), which could possibly be attributed to the indole interaction, indicating a preorientation of the *N*¹-acetamide substituent to undergo favorable interactions along the S1 pocket. The X-ray structure of the reference **2a** suggests that **2b** already connects substituents located in two adjacent pockets. This is supported by the fact that the corresponding fragment **1b** with the flexible ethanesulfonamide linker is significantly less active ($\Delta G = -14.4 \text{ kJ mol}^{-1}$), despite its similarity to **2b**. Moreover, the surprisingly low activity of the S4-directed fragments **1c**, **1d**, **2c**, **2d**, and **1e/2e** shows clearly that, although these moieties are highly privileged for full inhibitors, it would be unlikely that these groups could be identified by fragment screening.

Consequently, the fragment deconstruction of **1a** and **2a** allowed us to study detailed contributions to affinity, when growing molecules from their corresponding fragment into neighboring subsites. As expected, the most significant increase is observed, when S1 and S4 fragments are connected by appropriate linkers. These data on fXa inhibitors and fragments allows studying the influence of different linkers, as estimated from summing individual ΔG values for fragments **1** and **2** (ΔG_{frag1} , ΔG_{frag2}) and comparing them to the ΔG_{final} of the final inhibitor ($\Delta G_{\text{link}} = \Delta G_{\text{final}} - \Delta G_{\text{frag1}} - \Delta G_{\text{frag2}}$). Our analysis is summarized in Table 2; it reveals that linkers show different effects on the increase of ΔG_{link} .

Combining the chlorothiophene containing fragment **1g** ($\Delta G_{\text{frag1}} = -24.2 \text{ kJ mol}^{-1}$) with the S4 fragment **1d** ($\Delta G_{\text{frag2}} =$

$-11.4 \text{ kJ mol}^{-1}$) produces the original ligand **1a**, if only a single bond between both fragments is formed. The calculated affinity combining both fragments would thus be around $-35.6 \text{ kJ mol}^{-1}$, whereas a ΔG_{final} of $-49.6 \text{ kJ mol}^{-1}$ is observed. Thus, a high contribution of $\Delta G_{\text{link}} \approx -14.0 \text{ kJ mol}^{-1}$ can be attributed to the linker effect, which corresponds to an improvement by 2.5 orders of magnitude relative to individual affinities. This very high linker contribution ΔG_{link} suggests that no significant unfavorable interactions disturb the binding of this moiety. Table 2 shows the generation of **1a** and **2a** by combination of different fragments. Each combination leads to a very similar value for ΔG_{link} when generating **1a**. The deviations in ΔG_{link} observed for different combinations leading to **2a** results from the presence or absence of overlapping additional interactions of the fragments with the protein. For all cases leading to **1a**, a consistent ΔG_{link} value between -11.0 and $-14.2 \text{ kJ mol}^{-1}$ underscores the effectiveness of the flexible linker and highlights the usefulness of this decomposition approach. Consistently, related values for this combination are obtained. The smallest linker contribution of $-11.0 \text{ kJ mol}^{-1}$ is obtained for the combination of **1g** with **1b**, where the latter fragment in S4 already contains the S1-directed carboxamide and thus shows a slightly better affinity than **1c–e**. In contrast, replacing the sulfonamide by an amide in **1a** leads to **3** (Table 3) with a weaker affinity of $\Delta G = -34.8 \text{ kJ mol}^{-1}$; individual fragments **1g** and **2c** or **1g** and **2d** from deconstructing **3** account for -24.2 and $\gg -11.4 \text{ kJ mol}^{-1}$, respectively. This suggests no significant ΔG_{link} contribution of around $+0.8 \text{ kJ mol}^{-1}$, although individual fragments are as active as those for generating the lead structure **1a**. Hence, addition of a single acceptor to one fragment directed to S4 does not significantly influence the affinity, but has a dramatic net effect on the linker contribution of around $-11.8 \text{ kJ mol}^{-1}$, when comparing **1a** with **3**. Other explored linkers did not result in significant contributions.

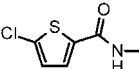
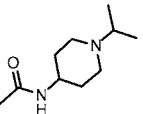
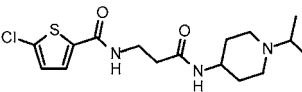
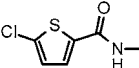
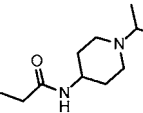
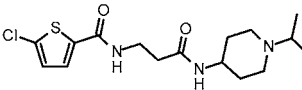
The fragment deconstruction of indole-2-carboxamides shows a similar trend with favorable contributions of ΔG_{link} between -8.3 and $-21.8 \text{ kJ mol}^{-1}$ for generating **2a** from **2f** and **2g** in S1 with all S4 fragments **2b**, **c**, **d**, **e**, **h**, and **i**, respectively. In particular, the combination of **2g** with **2h** represents the smallest structural change to arrive at the final compound **2a**; here the linker effect is -8.3 kJ mol^{-1} . Interestingly, the deconstruction of the rigid indole-2-carboxamide shows a smaller linking effect of -8.3 kJ mol^{-1} for those fragments **2g** and **2h**, which are combined to the final ligand **2a** with only minimal changes. This might indicate that this linker does not permit the S1 and S4 moieties to adopt optimal conformations. However, this energetic penalty is partially compensated by further interactions resulting in **2a**, which is equipotent to **1a**. Only for the combination of fragments **2g** and **2b**, an unfavorable linker effect ΔG_{link} of $+6.3 \text{ kJ mol}^{-1}$ indicates that fragment **2b** partially occupies the entrance of the fXa S1 pocket with its *N*¹-acetamide and thus connects both adjacent pockets. The acetamide is possibly H-bonded in S1, as in the X-ray structure of **2a**, while the indole might additionally contact flexible residues. Other combinations show a very pronounced linker effect.

Table 2: Combination of fragments 1 and 2 with experimental free energy of binding ΔG to generate factor Xa inhibitors 1a and 2a.^[a]

Fragment 1	Fragment 2		ΔG_{frag1}	ΔG_{frag2}	Final ligand	ΔG_{final}	$\Delta G_{\text{link}}^{[\text{b}]}$	Structural change	
	1g	1d	-24.2	-11.4		1a	-49.6	-14.0	add single bond
	1g	1c	-24.2	-11.4		1a	-49.6	-14.0	remove methyl
	1g	1b	-24.2	-14.4		1a	-49.6	-11.0	remove amide group
	1f	1e	-24.0	-11.4		1a	-49.6	-14.2	remove N-methyl
	1f	1c	-24.0	-11.4		1a	-49.6	-14.2	remove ethylsulfonylamide
	2g	2c	-20.0	-11.4		2a	-48.6	-17.2	add indole
	2g	2h	-20.0	-20.3		2a	-48.6	-8.3	remove methyl
	2g	2b	-20.0	-34.9		2a	-48.6	6.3	remove N-methylacetyl
	2f	2e	-25.8	-11.4		2a	-48.6	-11.4	remove N-methyl
	2f	2c	-25.8	-11.4		2a	-48.6	-11.4	remove propionamide
	2f	2d	-25.8	-11.4		2a	-48.6	-11.4	remove acetamide
	2i	2c	-15.4	-11.4		2a	-48.6	-21.8	remove 3 methyl groups
	2i	2d	-15.4	-11.4		2a	-48.6	-21.8	remove 2 methyl groups
	2i	2e	-15.4	-11.4		2a	-48.6	-21.8	add carbonyl

[a] Combination of fragments 1 and 2 results in a final ligand after minor structural changes as indicated. ΔG values are given in kJ mol^{-1} , they are calculated at 298 K. [b] The linker contributions are calculated using: $\Delta G_{\text{link}} = \Delta G_{\text{final}} - \Delta G_{\text{frag1}} - \Delta G_{\text{frag2}}$.

Table 3: Combination of fragments **1** and **2** with the experimental free-energy of binding ΔG to generate factor Xa inhibitor **3**.^[a]

Fragment 1	Fragment 2	ΔG_{frag1}	ΔG_{frag2}	Final ligand	$\Delta G_{\text{final}}^{[b]}$	$\Delta G_{\text{link}}^{[c]}$	Structural change
		1g	2d		-34.8	+0.8	add single bond
		1g	2c		-34.8	+0.8	remove methyl

[a] Combination of fragments **1** and **2** results in final ligand after minor structural changes indicated. ΔG values are given in kJ mol^{-1} , they are calculated at 298 K. [b] Compound **3** has a factor Xa inhibition K_i of $0.798 \mu\text{M}$. [c] The linker contribution is calculated using:

$$\Delta G_{\text{link}} = \Delta G_{\text{final}} - \Delta G_{\text{frag1}} - \Delta G_{\text{frag2}}$$

The favorable linker contribution of between -8.3 and $-21.8 \text{ kJ mol}^{-1}$ for both series is in very good agreement to ΔG_{link} estimation of $15\text{--}20 \text{ kJ mol}^{-1}$ by Murray and Verdonk.^[7] The values consistently obtained for different combinations are close to the estimated rigid body entropy barrier and thus indicate the presence of significant favorable linker effects and cooperative binding, when connecting fragments appropriately. This is especially true in the case of fragments **1g** and **1d**, where only a single bond is formed to give **1a**. In such a case, the increase in ΔG should be primarily due to the entropic gain of fragment linking as first approximation, if enthalpic interactions in fragments are maintained in the final ligand.^[8] These essential enthalpic interactions for **1a** and **2a** are revealed by X-ray structures, whereas the binding modes are presumed to be analogous to the final ligands.^[27]

In summary we have presented a comparative investigation of the linking effect by combining different scaffolds with congeneric fragments addressing two fXa subpockets. The systematic application of fragment deconstruction allowed us to estimate the linking coefficients for various fragment combinations and shows that a flexible 2-amino-ethanesulfonamide scaffold with a $\Delta G_{\text{link}} \approx -14.0 \text{ kJ mol}^{-1}$ is a nearly ideal linking moiety without any significant penalty because of unfavorable interactions. The variation of fragments in this context revealed linker contributions between -11.0 and $-14.2 \text{ kJ mol}^{-1}$. A related trend with linking contributions between -8.3 and $-21.8 \text{ kJ mol}^{-1}$ is also observed for the indole-2-carboxamide-based fXa inhibitor. Interestingly, the deconstruction of the rigid indole-2-carboxamide displayed a lower linking effect of -8.3 kJ mol^{-1} for **2g** and **2h**, which are combined to **2a** with minimal structural changes. This linking element does not permit the S1 and S4 binding moieties to adopt their optimal conformations. However, this energetic price is at least partially compensated by addressing further secondary interactions along the binding pockets resulting in **2a** which is equipotent to **1a**. Thus, the introduction of rigid aromatic moieties as a common approach to increase affinity does not necessarily maximize the benefit from the linker effect as detrimental affinity contributions might originate from suboptimal orientation and accommodation of specific binding elements. Furthermore, the weak activity of S4 fragments in this study indicates that, although these moieties are privileged and optimal for full inhibitors, it would be

unlikely that they could be identified by fragment screening. This deconstruction procedure is a useful strategy for exploring the binding characteristics and opportunities for a given lead structure which can highlight cooperative effects in protein–ligand interactions. It also reveals the favorable effect of linking two privileged fragments with minimal or no structural changes on binding affinity.

Received: October 6, 2011

Revised: November 22, 2011

Published online: December 21, 2011

Keywords: additivity · drug discovery · fragment linking · molecular recognition · noncovalent interactions

- [1] P. A. Rejto, G. M. Verkhivker, *Proc. Natl. Acad. Sci. USA* **1996**, 93, 8945–8950.
- [2] a) A. L. Hopkins, C. R. Groom, A. Alex, *Drug Discovery Today* **2004**, 9, 430–431; b) C. Abad-Zapatero, *Expert Opin. Drug Discovery* **2007**, 2, 469–488; c) D. C. Rees, M. Congreve, C. W. Murray, R. Carr, *Nat. Rev. Drug Discovery* **2004**, 3, 660–672; d) E. Perola, *J. Med. Chem.* **2010**, 53, 2986–2997.
- [3] a) M. Congreve, G. Chessari, D. Tisi, A. J. Woodhead, *J. Med. Chem.* **2008**, 51, 3661–3680; b) P. J. Hajduk, J. Greer, *Nat. Rev. Drug Discovery* **2007**, 6, 211–219.
- [4] D. A. Erlanson, J. A. Wells, A. C. Braisted, *Annu. Rev. Biophys. Biomol. Struct.* **2004**, 33, 199–223.
- [5] M. I. Page, W. P. Jencks, *Proc. Natl. Acad. Sci. USA* **1971**, 68, 1678–1683.
- [6] S. B. Shuker, P. J. Hajduk, R. P. Meadows, S. W. Fesik, *Science* **1996**, 274, 1531–1534.
- [7] C. W. Murray, M. L. Verdonk, *J. Comput.-Aided Mol. Des.* **2002**, 16, 741–753.
- [8] a) K. A. Dill, *J. Biol. Chem.* **1997**, 272, 701–704; b) A. E. Mark, W. F. van Gunsteren, *J. Mol. Biol.* **1994**, 240, 167–176; c) B. Baum, L. Muley, M. Smolinski, A. Heine, D. Hangauer, G. Klebe, *J. Mol. Biol.* **2010**, 397, 1042–1054.
- [9] V. Borsi, V. Calderone, M. Fragai, C. Luchinat, N. Sarti, *J. Med. Chem.* **2010**, 53, 4285–4289.
- [10] E. T. Olejniczak, P. J. Hajduk, P. A. Marcotte, D. G. Nettlesheim, R. P. Meadows, E. Edalji, T. F. Holzman, S. W. Fesik, *J. Am. Chem. Soc.* **1997**, 119, 5828–5832.
- [11] We analyzed these examples in the same way as described for factor Xa ligands **1a** and **2a** and the results have been added to the Supporting Information (Table S1) for comparison. Only for some cases a significant favorable linker contribution ΔG_{link} has

been reported. This first case relates to a small sulfonamide-based MMP-12 inhibitor combined from two small fragments AHA (acetoxyhydroxamic acid) and PMS (*para*-methoxy benzenesulfonamide). Here, a favorable linking coefficient ΔG_{link} of $-15.2 \text{ kJ mol}^{-1}$ was observed (Table S1). This is due to a favorable entropic contribution, whereas the enthalpic term is similar to the sum of both fragments. The linking of AHA (Olej1) with another biaryl substituent (Olej3) by a single bond to generate MMP-3 inhibitors resulted in a reduced, but still favorable linker coefficient of -6.5 kJ mol^{-1} . The extreme case represents without question the formation of streptavidin from individual fragments by connecting two fragments by a single bond, which results in a ΔG_{link} of $-24.7 \text{ kJ mol}^{-1}$ because of the superior binding affinity of streptavidin.

- [12] K. Babaoglu, B. K. Shoichet, *Nat. Chem. Biol.* **2006**, *2*, 720–723.
- [13] M. Nazaré, D. W. Will, H. Matter, H. Schreuder, K. Ritter, M. Urmann, M. Essrich, A. Bauer, M. Wagner, J. Czech, M. Lorenz, V. Laux, V. Wehner, *J. Med. Chem.* **2005**, *48*, 4511–4525.
- [14] M. Wagner, M. Urmann, V. Wehner, M. Lorenz, A. Bauer, M. Nazaré, H. Matter, WO 2006122661, **2006**.
- [15] S. Maignan, V. Mikol, *Curr. Top. Med. Chem.* **2001**, *1*, 161–174.
- [16] H. Matter, M. Nazaré, S. Güssregen, D. W. Will, H. Schreuder, A. Bauer, M. Urmann, K. Ritter, M. Wagner, V. Wehner, *Angew. Chem.* **2009**, *121*, 2955–2960; *Angew. Chem. Int. Ed.* **2009**, *48*, 2911–2916.
- [17] H. Matter, D. W. Will, M. Nazaré, H. Schreuder, V. Laux, V. Wehner, *J. Med. Chem.* **2005**, *48*, 3290–3312.
- [18] a) T. J. Tucker, S. F. Brady, W. C. Lumma, S. D. Lewis, S. J. Gardell, A. M. Naylor-Olsen, Y. Yan, J. T. Sisko, K. J. Stauffer, B. J. Lucas, J. J. Lynch, J. J. Cook, M. T. Stranieri, M. A. Holahan, E. A. Lyle, E. P. Baskin, I. W. Chen, K. B. Dancheck, J. A. Krueger, C. M. Cooper, J. P. Vacca, *J. Med. Chem.* **1998**, *41*, 3210–3219; b) M. Adler, M. J. Kochanny, B. Ye, G. Rumennik, D. R. Light, S. Biancalana, M. Whitlow, *Biochemistry* **2002**, *41*, 15514–15523; c) M. T. Stubbs, S. Reyda, F. Dullweber, M. Moller, G. Klebe, D. Dorsch, W. W. K. R. Mederski, H. Wurziger, *ChemBioChem* **2002**, *3*, 246–249; d) S. Maignan, J.-P. Guilloteau, Y. M. Choi-Sledeski, M. R. Becker, W. R. Ewing, H. W. Pauls, A. P. Spada, V. Mikol, *J. Med. Chem.* **2003**, *46*, 685–690; e) S. Roehrig, A. Straub, J. Pohlmann, T. Lampe, J. Pernerstorfer, K.-H. Schlemmer, P. Reinemer, E. Perzborn, *J. Med. Chem.* **2005**, *48*, 5900–5908; f) M. J. Hartshorn, C. W. Murray, A. Cleasby, M. Frederickson, I. J. Tickle, H. Jhoti, *J. Med. Chem.* **2005**, *48*, 403–413; g) Y. Shi, D. Sitkoff, J. Zhang, H. E. Klei, K. Kish, E. C.-K. Liu, K. S. Hartl, S. M. Seiler, M. Chang, C. Huang, S. Youssef, T. E. Steinbacher, W. A. Schumacher, Y. Grazier, A. Pudzianowski, A. Apedo, L. Doscenza, J. Yanchunas, P. D. Stein, K. S. Atwal, *J. Med. Chem.* **2008**, *51*, 7541–7551; h) A. Straub, S. Roehrig, A. Hillisch, *Curr. Top. Med. Chem.* **2010**, *10*, 257–269.
- [19] M. Nazaré, M. Essrich, D. W. Will, H. Matter, K. Ritter, M. Urmann, A. Bauer, H. Schreuder, J. Czech, M. Lorenz, V. Laux, V. Wehner, *Bioorg. Med. Chem. Lett.* **2004**, *14*, 4197–4201.
- [20] P. Gallivan, D. A. Dougherty, *Proc. Natl. Acad. Sci. USA* **1999**, *96*, 9459–9464.
- [21] L. M. Salonen, C. Bucher, D. W. Banner, W. Haap, J.-L. Mary, J. Benz, O. Kuster, P. Seiler, W. B. Schweizer, F. Diederich, *Angew. Chem.* **2009**, *121*, 825–828; *Angew. Chem. Int. Ed.* **2009**, *48*, 811–814.
- [22] K. Schärer, M. Morgenthaler, R. Paulini, U. Obst-Sander, D. W. Banner, D. Schlatter, J. Benz, M. Stihle, F. Diederich, *Angew. Chem.* **2005**, *117*, 4474–4479; *Angew. Chem. Int. Ed.* **2005**, *44*, 4400–4404.
- [23] D. J. P. Pinto, J. M. Smallheer, D. L. Cheney, R. M. Knabb, R. R. Wexler, *J. Med. Chem.* **2010**, *53*, 6243–6274.
- [24] a) Calculated pK_a of 10.1 using the program MoKa (Molecular Discovery Ltd., version 1.1.0); b) F. Milletti, L. Storchi, G. Sforna, G. Cruciani, *J. Chem. Inf. Model.* **2007**, *47*, 2172–2181; c) F. Milletti, L. Storchi, L. Goracci, S. Bendels, B. Wagner, M. Kansy, G. Cruciani, *Eur. J. Med. Chem.* **2010**, *45*, 4270–4279.
- [25] A. Ciulli, G. Williams, A. G. Smith, T. L. Blundell, C. Abell, *J. Med. Chem.* **2006**, *49*, 4992–5000.
- [26] S. Barelier, J. Pons, O. Marcillat, J.-M. Lancelin, I. Krimm, *J. Med. Chem.* **2010**, *53*, 2577–2588.
- [27] C. McMartin, R. S. Bohacek, *J. Comput.-Aided Mol. Des.* **1997**, *11*, 333–344.
- [28] a) W. Heiden, T. Goetze, J. Brickmann, *J. Comput. Chem.* **1993**, *14*, 246–250; b) Color code for the hydrogen-bonding potential. Blue: ligand–donor favorable, red: ligand–acceptor favorable.